Supporting Information

Hierarchically porous Ni foam-supported Co and Sn doped Ni_3S_2 nanosheets for oxygen evolution reaction electrocatalysts

Won Young An [a, £], Hyungwoo Lee [b, £], Sung Ryul Choi [a], Sungyong Choi [a], Hyun-Seok Cho [c], Minseok Choi [b, *], Jun-Young Park [a, *]

[a] *HMC, Department of Nanotechnology and Advanced Materials Engineering, Sejong University, Seoul 05006, Korea*

[b] *Department of Physics, Inha University, Incheon 22212, Korea*

[c] *Polymer Electrolyte Fuel Cell Research Center, Hydrogen and Fuel Cell Department, Korea Institute of Energy Research (KIER), Daejeon 34129, Korea*

[£] Won Young An and Hyungwoo Lee contributed equally as first authors.

***** Correspondence and requests for materials should be addressed to J.-Y. Park (email: jyoung@sejong.ac.kr; Tel: +82-2-3408-3848) and Minseok Choi **(**email: minseokchoi.phd@gmail.com).

Table S1. Characterization data of pristine and doped-Ni_3S_2@NF (annealed at 160 °C for 4 h) catalysts from N_2 adsorption analysis.

Catalysts	BET surface area ($m^2 \cdot g^{-1}$)	Mean pore diameter (nm)	Total pore volume ($cm^3 \cdot g^{-1}$)
Ni_3S_2@NF	4.56	14.3	0.016
Co-Ni_3S_2@NF	7.26	9.4	0.018
CoNi-Ni_3S_2@NF	7.66	7.2	0.014
CoFe-Ni_3S_2@NF	6.34	7.1	0.011
CoSn-Ni_3S_2@NF	7.66	6.2	0.015

Table S2. Performance comparison of the CoSn-Ni_3S_2@NF OER anodic catalyst in electrolysis cell with the previously reported anodic materials.

Anode catalysts	Membrane// cathode	Electrolyte (temperature, °C)	Cell voltage (V)	Current density (A cm^{-2})
CoSn-Ni_3S_2@NF (this work)	FAA-3-50// NiFe-LDH	1 M KOH (55)	2.0	1.367
	Zirfon// NiFe-LDH	30 wt.% KOH (80)	2.0	0.643
$CuCoO_x$@NF[1]	FAA-3// Ni/(CeO_2-La_2O_3)/C	1% K_2CO_3 (60)	1.95	0.5
$CuCoO_x$@NF[1]	Tokuyama(A-201)// Ni/(CeO_2-La_2O_3)/C	1 M KOH (60)	1.88	0.4
Co_2Fe_1[2]	FAA-3// Pt/C	1 M KOH (none)	1.8	0.13
$NiCoFeO_x$[3]	FFA-3// Pt/C	Nanopure water (50)	2.3	1.0
g-CN-CNF[4]	FAA-3-50// Pt/C	1 M KOH (60)	1.9	0.734
$Cu_xCo_{3-x}O_4$[5] (Co/Cu =1.8)	FAA-3-50// Ni film	1 M KOH (70)	2.2	0.11
Ni/carbon paper[6]	Tokuyama(A-201)// Ni	1 M KOH (50)	1.9	0.15
NiCoTi@Ti foil[7]	Tokuyama(A-201)// NiCoTi@Ti foil	1 M KOH (none)	2.0	0.17

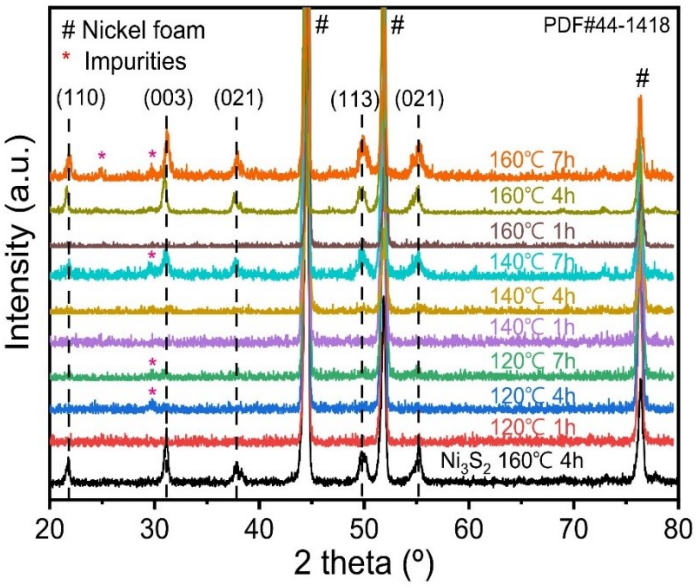

Fig. S1. XRD patterns of Co-Ni_3S_2@NF catalysts synthesized under various hydrothermal processing conditions (temperature = 120, 140, and 160 °C and time = 1, 4, and 7 h).

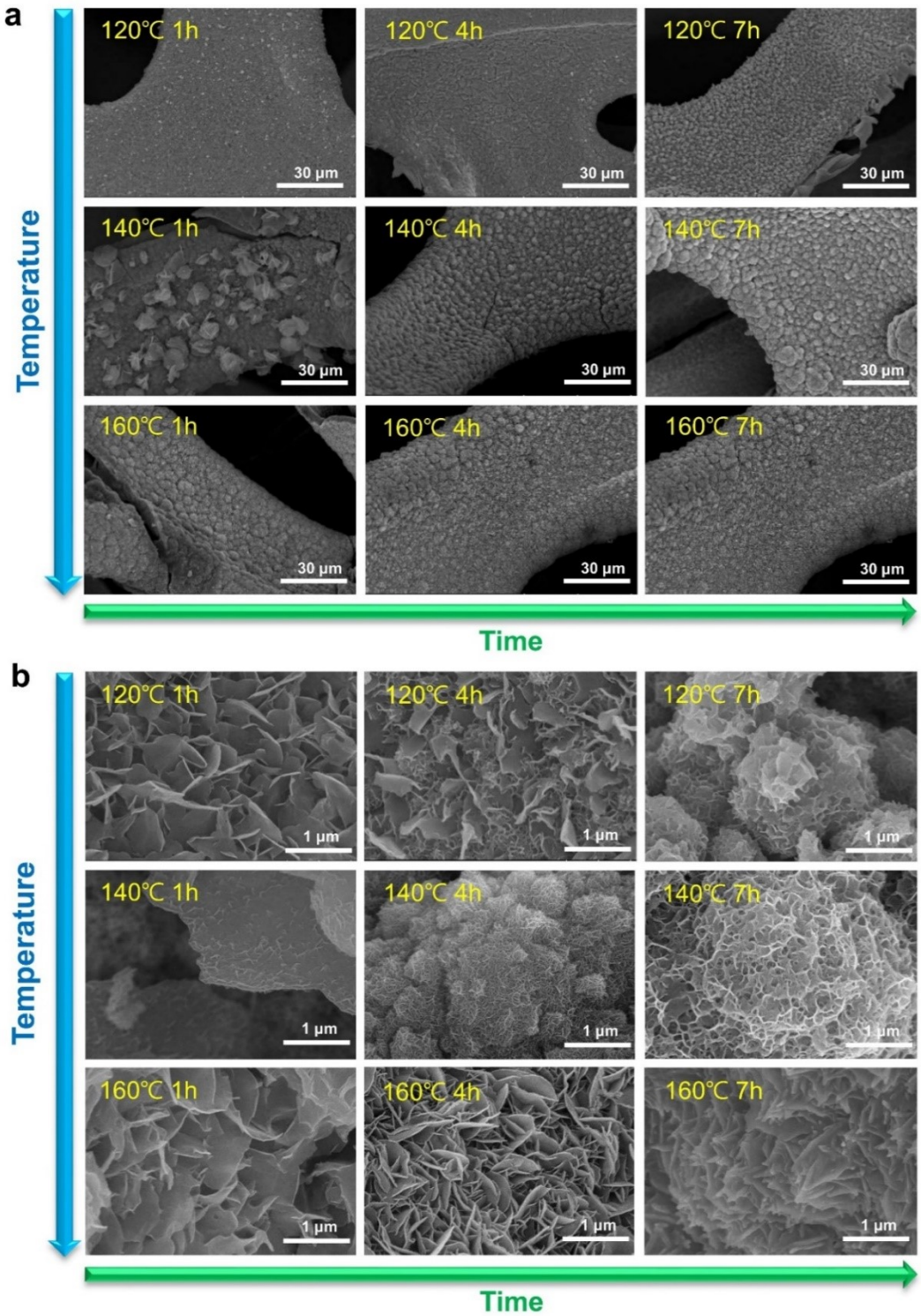

Fig. S2. FE-SEM image of Co-Ni_3S_2@NF catalysts synthesized under various hydrothermal processing conditions. a) Low magnification. b) High magnification.

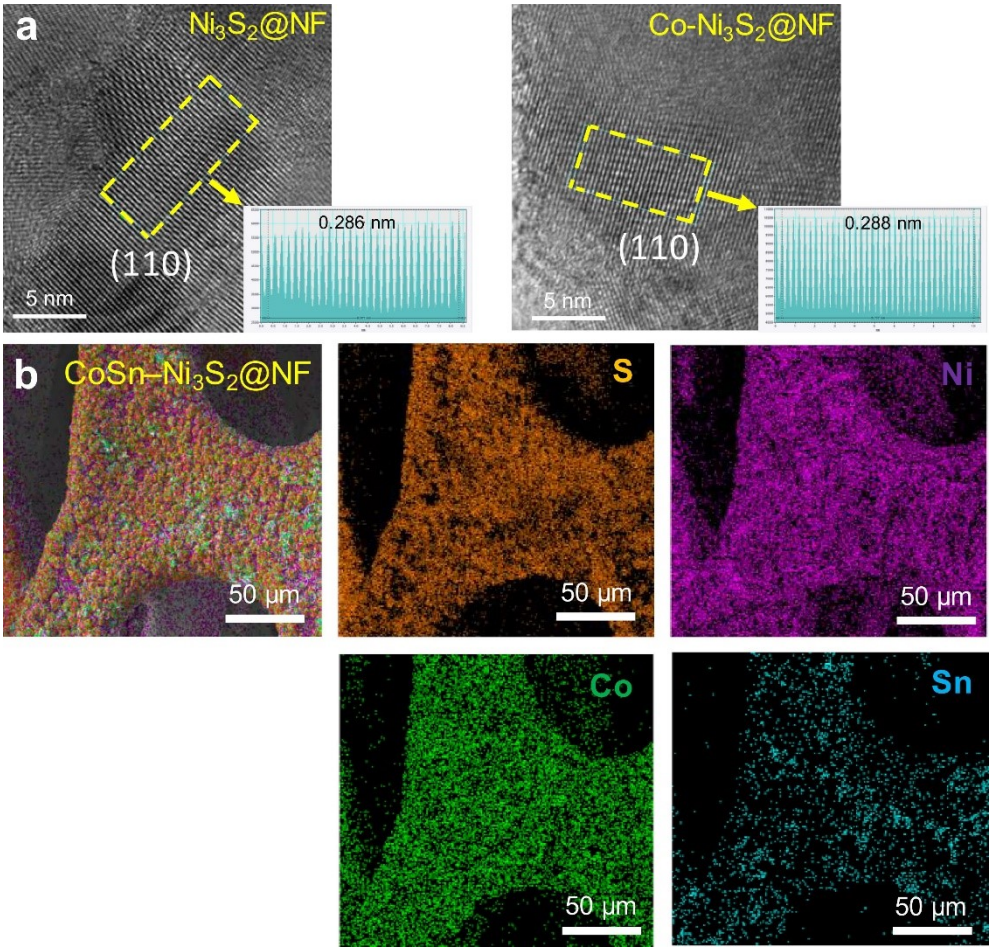

Fig. S3. Physicochemical analysis of catalysts. (a) HRTEM atomic resolution images of Ni_3S_2@NF and Co-Ni_3S_2@NF. (b) EDX elemental mapping results of CoSn-Ni_3S_2@NF (elements = S, Ni, Co, and Sn).

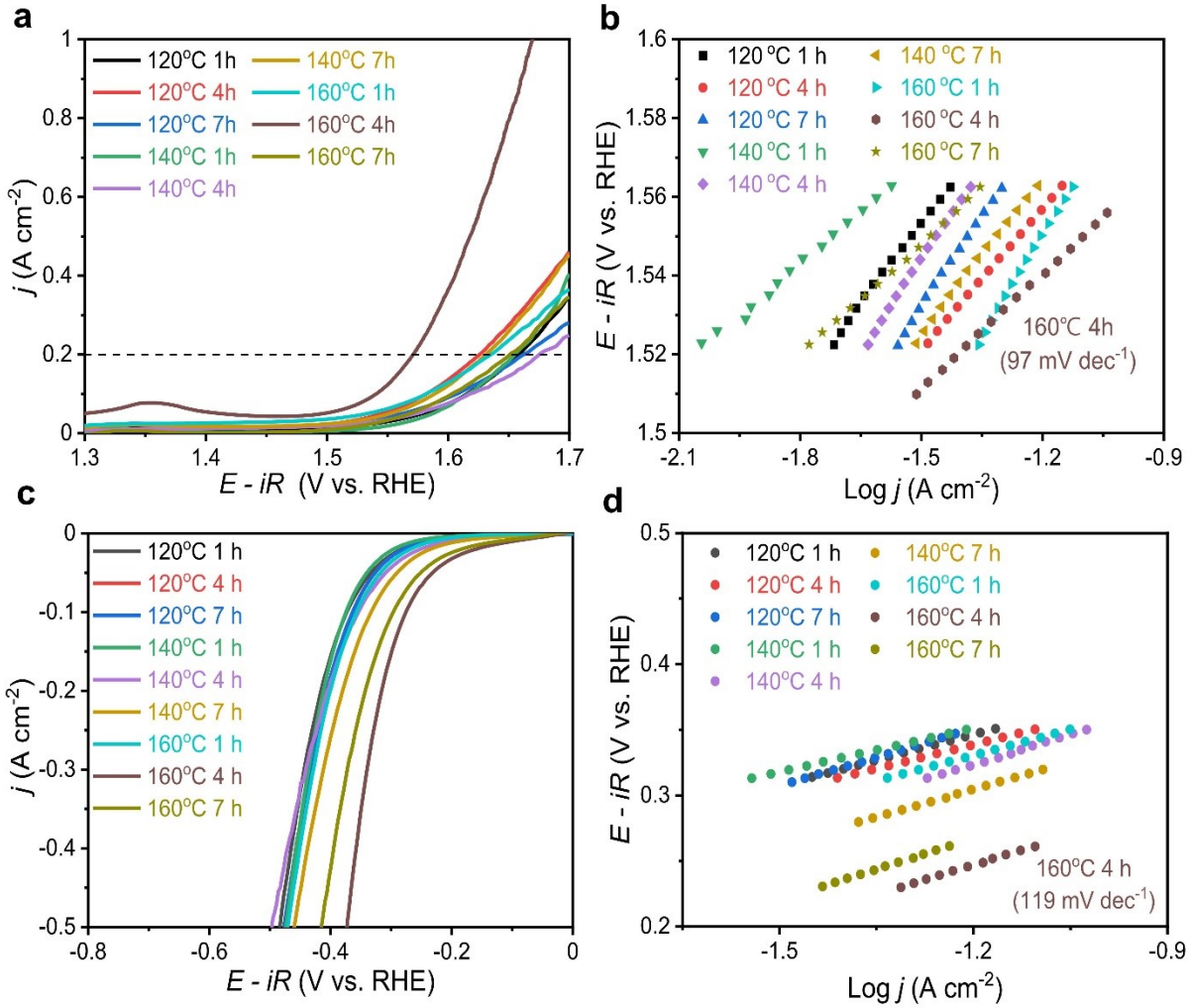

Fig. S4. OER and HER polarization curves of Co-Ni_3S_2@NF catalysts synthesized under various hydrothermal processing conditions. a) OER activity curves and b) corresponding Tafel plots for Co-Ni_3S_2@NF catalysts. c) HER activity curves and d) corresponding Tafel plots for Co-Ni_3S_2@NF catalysts.

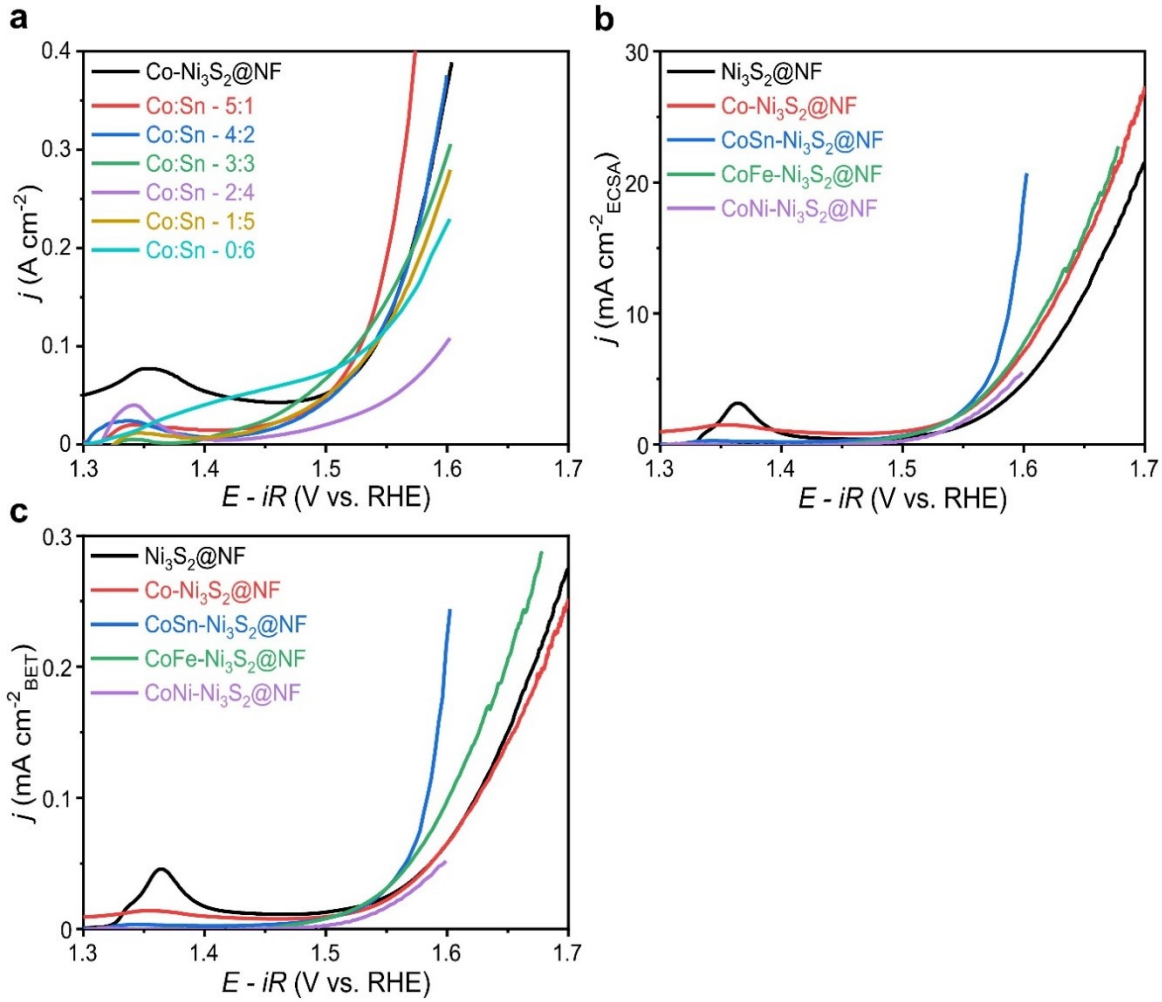

Fig. S5. OER polarization curves of transition and post transition metal-doped Ni_3S_2@NF catalysts. a) *j-V* curves of Co_xSn_y-Ni_3S_2@NF with different ratios of Co and Sn. b–c) *j-V* curves of doped-Ni_3S_2@NF catalysts normalized by ECSA (b) and BET (c).

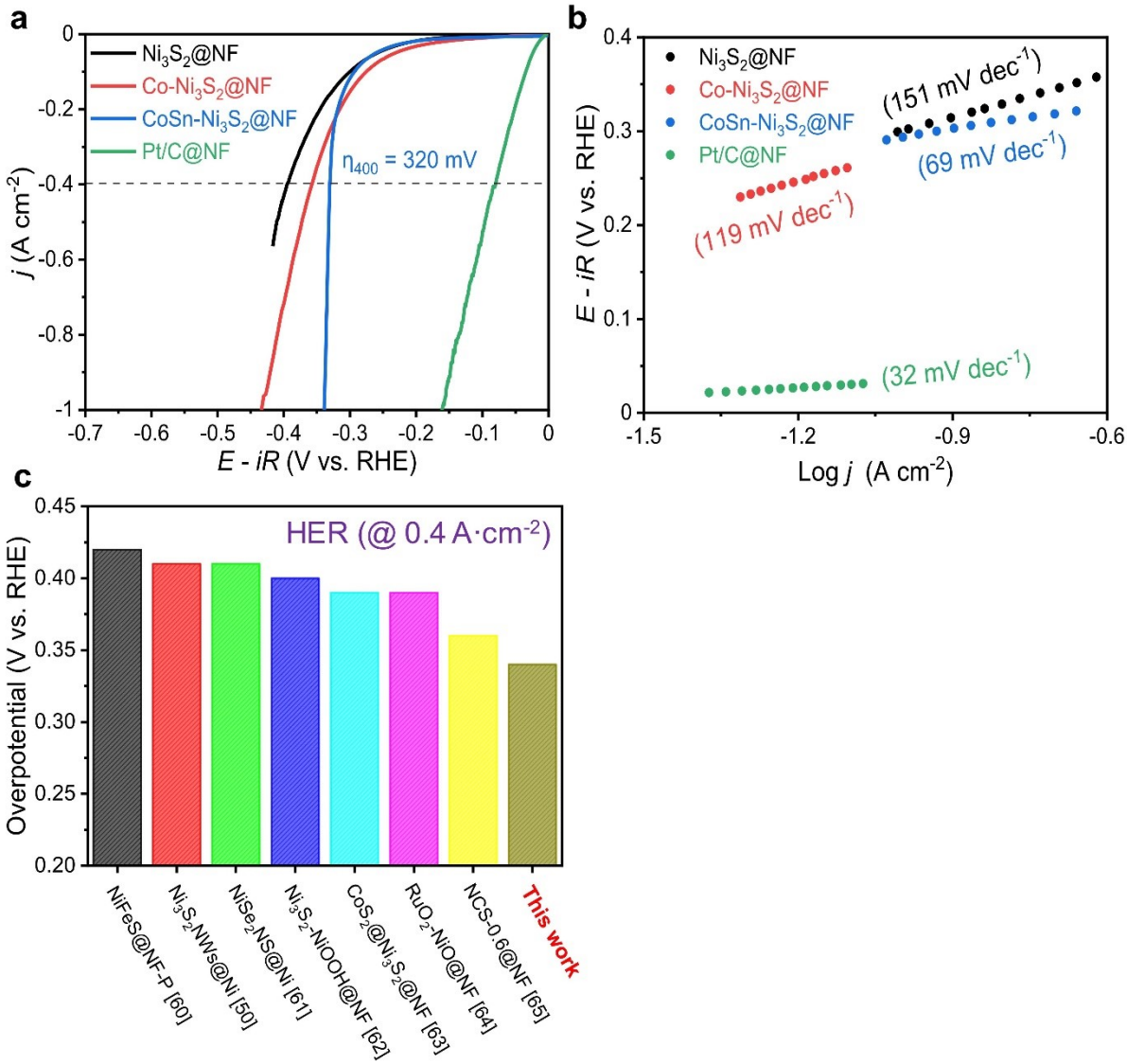

Fig. S6. HER polarization curves of Ni_3S_2@NF, Co-Ni_3S_2@NF, CoSn-Ni_3S_2@NF, and Pt/C catalysts. a) HER activity curves and b) corresponding Tafel plots of catalysts. c) Comparison of overpotential (η) at 0.4 A·cm^{-2} for CoSn-Ni_3S_2@NF with previously reported results for other nickel-based catalysts.

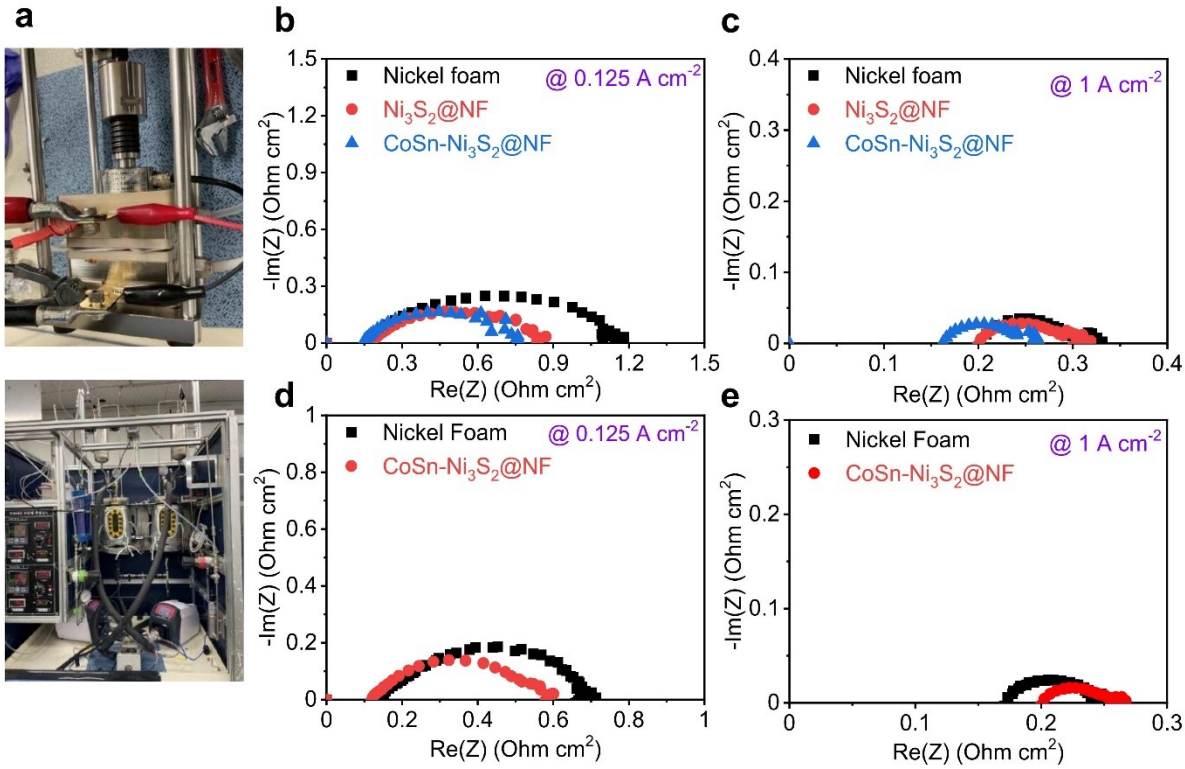

Fig. S7. Experimental setup and electrochemical results of alkaline water-splitting cells (with NF, Ni_3S_2@NF, and CoSn-Ni_3S_2@NF electrodes). a) Electrolysis experimental setup with a single cell zero-gap configuration composed of Ni porous transport layers, bipolar plates, and a membrane separator. b–c) EIS curves of alkaline water-splitting cells at 0.125 A·cm^{-2} (b) and 1 A·cm^{-2} (c) in 1 M KOH solution at 55 °C. d–e) EIS curves of alkaline water-splitting cells at 0.125 A·cm^{-2} (d) and 1 A·cm^{-2} (e) in 30 wt.% KOH solution at 80 °C.

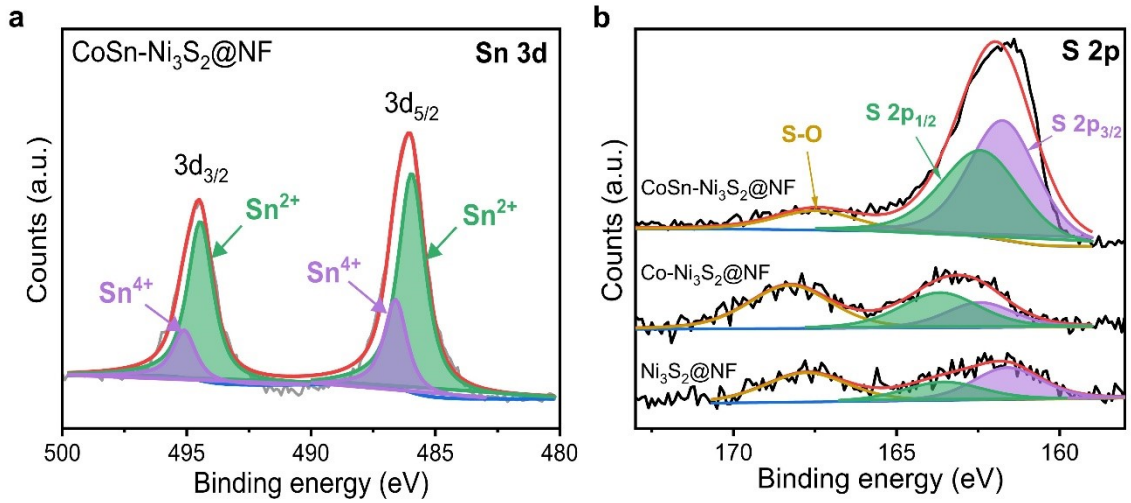

Fig. S8. XPS spectra of a) Sn 3*d* and b) S 2*p* peaks of catalysts (Ni_3S_2@NF, Co-Ni_3S_2@NF, and CoSn-Ni_3S_2@NF).

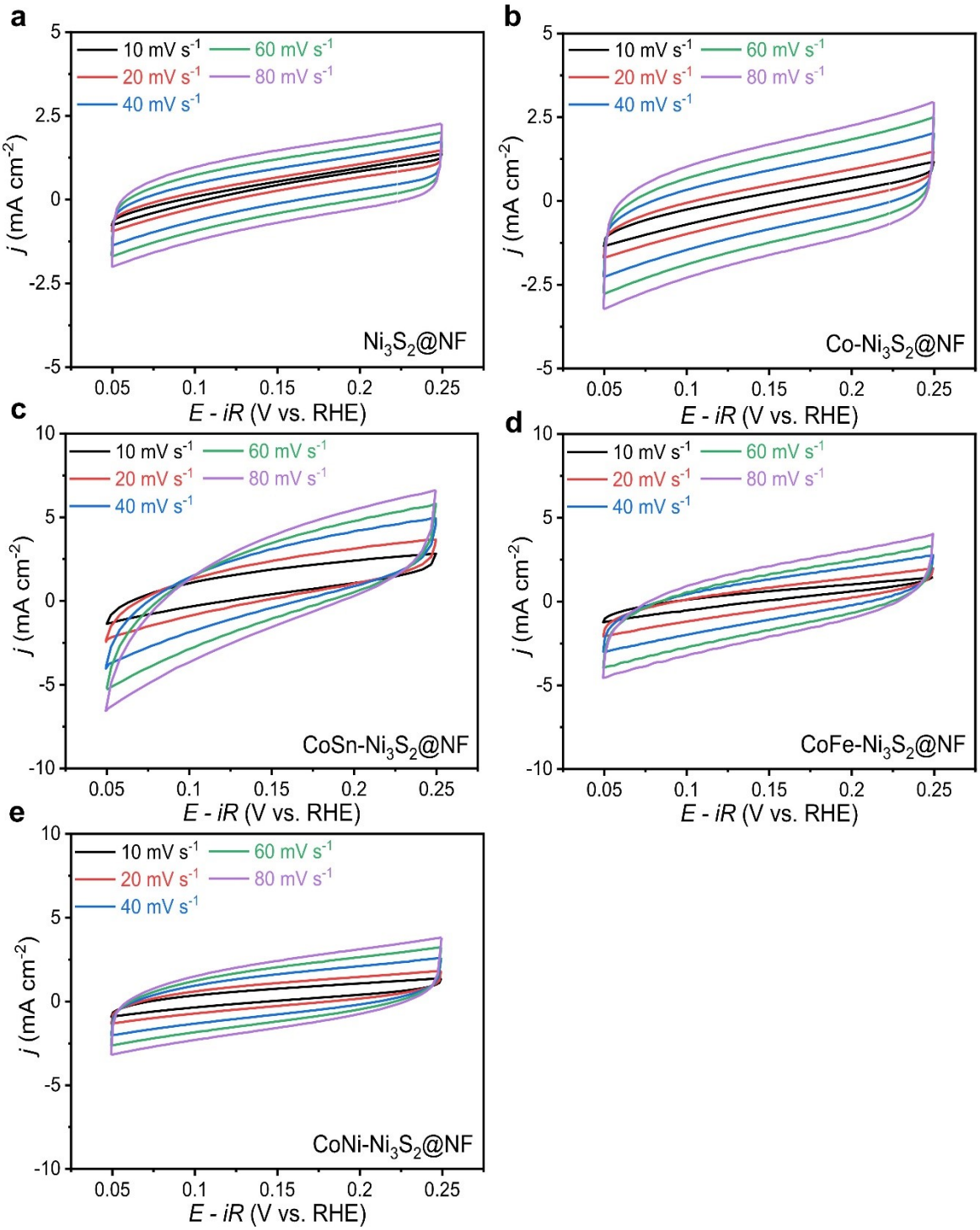

Fig. S9. Cyclic voltammograms (CVs, 0.05 – 0.25 V *vs.* RHE) of catalysts with various scan rates (10, 20, 40, 60, and 80 mV·s^{-1}). a) Ni_3S_2@NF, b) Co-Ni_3S_2@NF, c) CoSn-Ni_3S_2@NF, d) CoFe-Ni_3S_2@N, and e) CoNi-Ni_3S_2@NF.

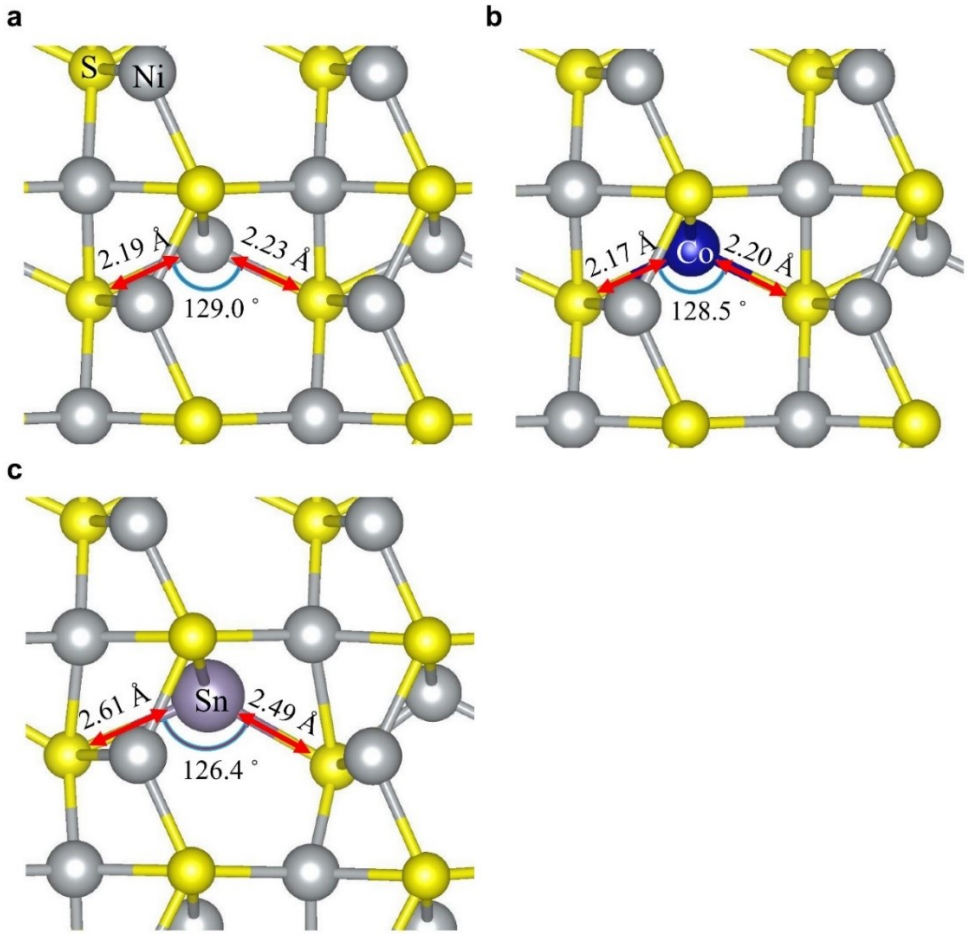

Fig. S10. Local atomic structure obtained using DFT calculations. a) Ni_3S_2, b) Co-Ni_3S_2, and c) Sn-Ni_3S_2.

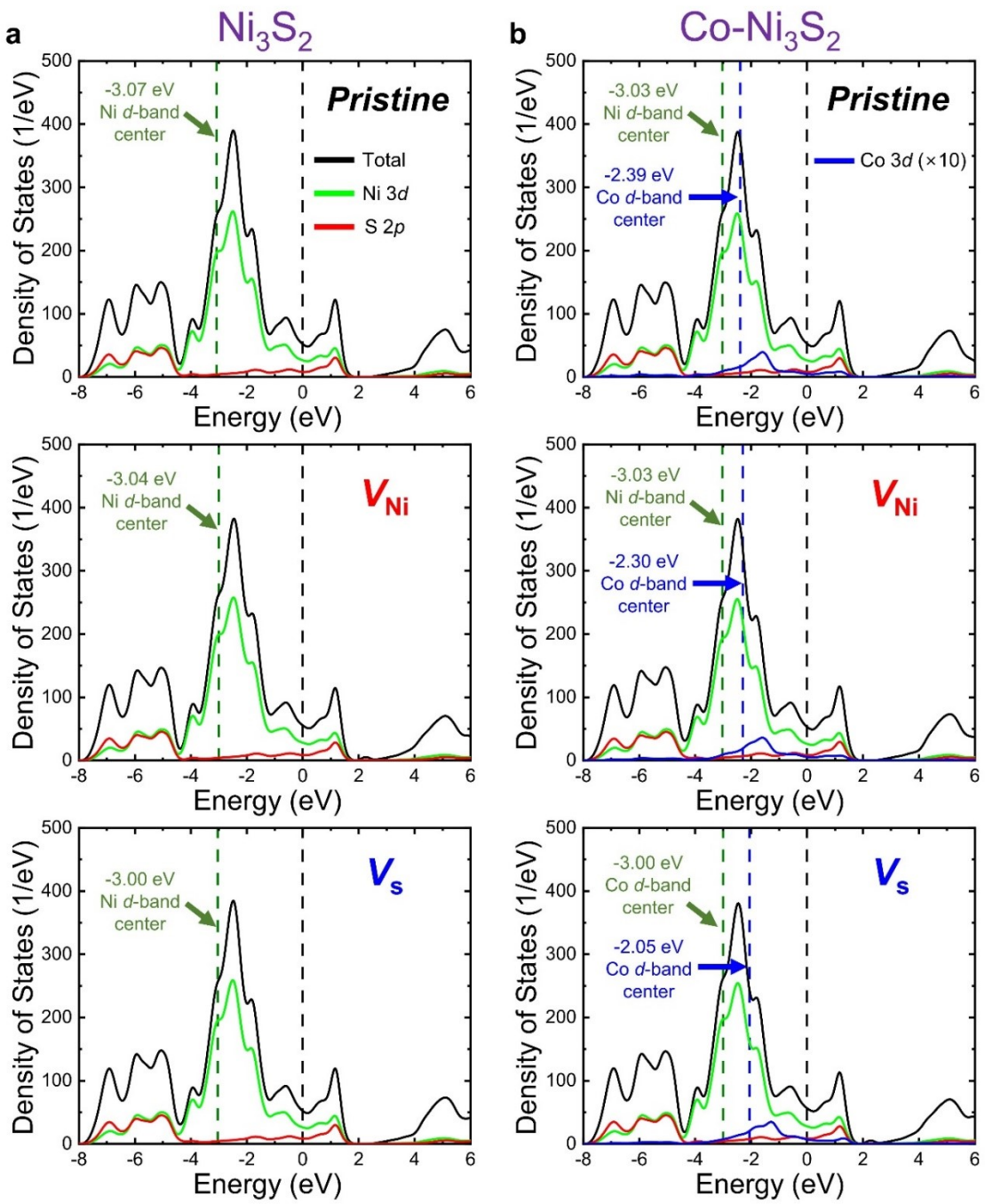

Fig. S11. Density of states (DOS) of a) Ni_3S_2 and b) Co-Ni_3S_2 obtained using DFT calculations. V_{Ni} and V_S are responsible for the DOS of the systems including V_{Ni} and V_S, respectively. Olive and blue dashed lines denote Ni 3*d*-band center and Co 3*d*-band center, respectively, and black line indicates Fermi level. DOS values of the Co components are multiplied by ten for easy visualization.

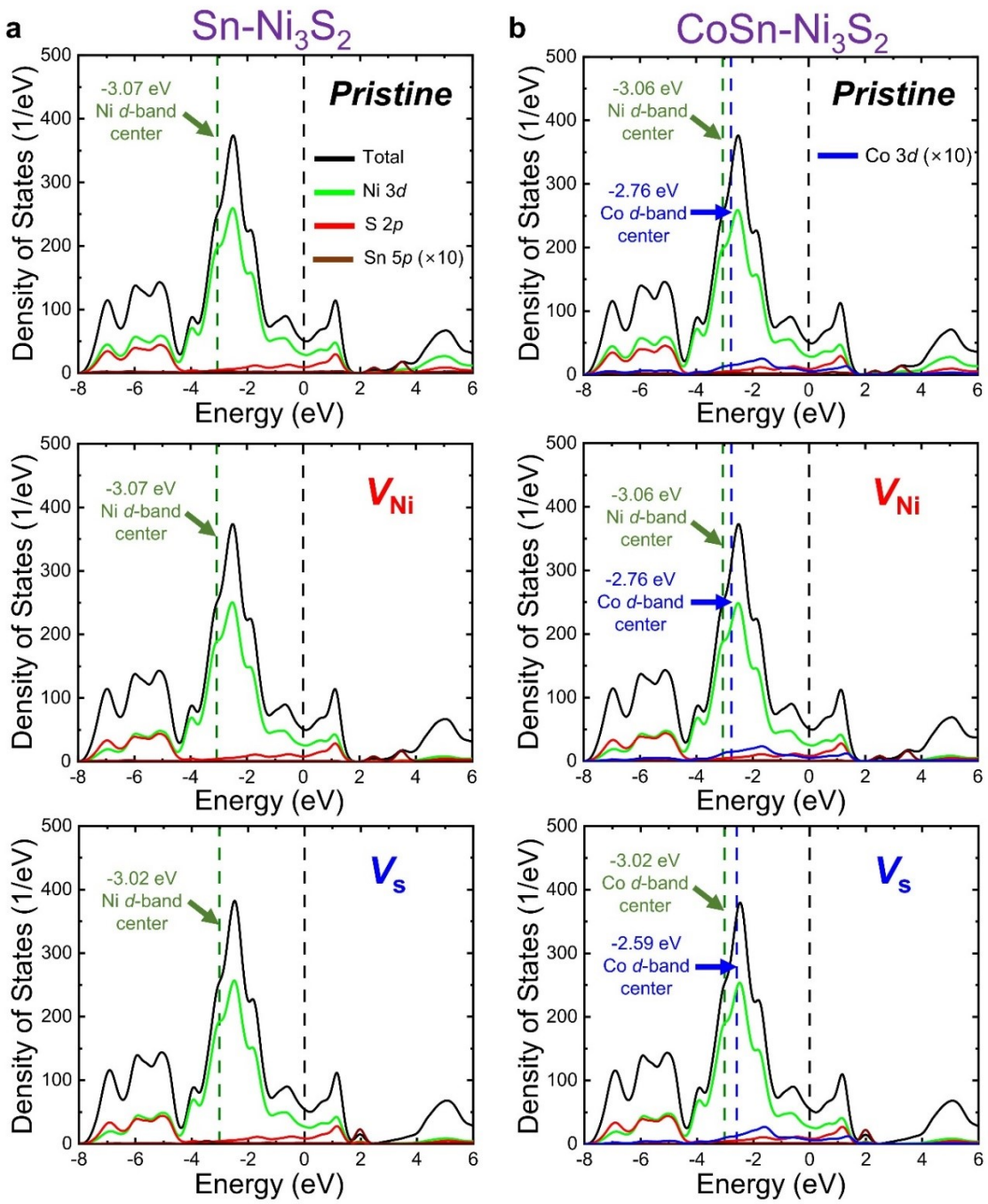

Fig. S12. Density of states (DOS) of a) Sn-Ni_3S_2 and b) CoSn-Ni_3S_2 obtained using DFT calculations. V_{Ni} and V_S are responsible for the DOS of the systems including V_{Ni} and V_S, respectively. Olive and blue dashed lines denote Ni 3*d*-band center and Co 3*d*-band center, respectively, and black line indicates Fermi level. DOS values of the Co and Sn components are multiplied by ten for easy visualization.

References

1. I. Vincent, A. Kruger, D. Bessarabov, *Int. J. Hydrog. Energy*, 2017, **42**, 10752–10761.
2. G.-C. Chen, T. H. Wondimu, H.-C. Huang, K.-C. Wang, C. H. Wang, *Int. J. Hydrog. Energy*, 2019, **44**, 10174–10181.
3. D. Xu, M. B. Stevens, M. R. Cosby, S. Z. Oener, A. M. Smith, L. J. Enman, K. E. Ayers, C. B. Capuano, J. N. Renner, N. Danilovic, Y. Li, H. Wang, Q. Zhang, S. W. Boettcher, *ACS Catal.*, 2019, **9**, 7–15.
4. J. E. Park, M.-J. Kim, M. S. Lim, S. Y. Kang, J. K. Kim, S.-H. Oh, M. Her, Y.-H. Cho, Y.-E. Sung, *Appl Catal B: Environ.*, 2018, **237**, 140–148.
5. E. López-Fernández, J. Gil-Rostra, J. P. Espinós, A. R. González-Elipe, F. Yubero, A. de Lucas-Consuegra, *J. Power Sources*, 2019, **415**, 136–144.
6. S. H. Ahn, B. S. Lee, I. Choi, S. J. Yoo, H. J. Kim, E. Cho, D. Henkensmeier, S. W. Nam, S. K. Kim, J. H. Jang, *Appl. Catal. B*, 2014, **154**, 197–205.
7. P. Ganesan, A. Sivanantham, S. Shanmugam, *ACS Appl. Mater. Interfaces*, 2017, **9**, 12416–12426.